Physica A 432 (2015) 156–166

Contents lists available at ScienceDirect

Physica A

journal homepage: www.elsevier.com/locate/physa

Effects of surface topography on the collective diffusion of interacting adsorbed particles

M.E.R. Rodríguez, P.M. Pasinetti, F. Bulnes, A.J. Ramirez-Pastor *

Departamento de Física, Instituto de Física Aplicada (INFAP), Universidad Nacional de San Luis, CONICET, Chacabuco 917, D5700BWS, San Luis, Argentina

HIGHLIGHTS

- Collective diffusion of interacting particles adsorbed on heterogeneous surfaces.
- Bivariate surface of adsorptive patches with a characteristic correlation length l.
- A rich variety of structural orderings were observed in the adlayer.
- Transport coefficients are strongly affected by surface topography and ad–ad couplings.

ARTICLE INFO

Article history:
Received 22 December 2014
Received in revised form 17 March 2015
Available online 26 March 2015

Keywords:
Diffusion
Adsorption
Heterogeneous surfaces
Monte Carlo simulations

ABSTRACT

Collective diffusion of particles with repulsive nearest-neighbor interactions on bivariate surfaces is studied through Monte Carlo simulation, in the framework of the Kubo–Green theory. Shallow and deep adsorbing sites form $l \times l$ patches distributed at random or in chessboard-like ordered domains on a two-dimensional square lattice. The influence of the energetic correlation and the lateral interactions on the jump and collective diffusion coefficients are analyzed by simulating the coverage fluctuations in the grand canonical ensemble and the mean-square displacements of particles in the canonical ensemble. The combination of topography and lateral coupling is shown to produce interesting effects such as different filling regimes as well as strong effects on the coverage dependence of the transport coefficients.

1. Introduction

The role of the adsorptive surface characteristics in many processes of practical importance is a topic of increasing interest in surface science [1–4]. Most materials have heterogeneous surfaces which, when interacting with gas molecules, present a complex spatial dependence of the adsorptive energy. This property, called surface topography, affects strongly many molecular processes occurring on such surfaces, like adsorption, surface diffusion and reactions, thus making the simple determination of the adsorptive energy distribution (AED) not enough to characterize the heterogeneity [5]. It is then necessary to obtain the multivariate probability distribution, or at least the AED plus the spatial correlation function. This is a formidable and still unsolved problem.

Diffusion of adsorbates is a much demanding problem both experimentally and theoretically [6–9]. It is worth to mention some recent theoretical contributions [8,9] where, using a variational method, interesting properties in the collective motion of the particles were found. These studies were carried out in a one-dimensional system of random wells and barriers, as well

* Corresponding author.
E-mail address: antorami@unsl.edu.ar (A.J. Ramirez-Pastor).

http://dx.doi.org/10.1016/j.physa.2015.03.025
0378-4371/

as in simple systems of square and hexagonal symmetry. However, for more general systems some further approximations have to be introduced to this approach.

One way of overcoming these theoretical and experimental complications is to use Monte Carlo (MC) simulation method. MC technique is a valuable tool for studying surface molecular phenomena, which has been extensively used to simulate many different diffusion processes including fractal substrates [10,11], cavities [12], multisite occupancy [13,14] and phase transitions [15–20].

Among the contributions addressing MC simulation of surface diffusion, Refs. [21–23] are especially interesting to contextualize the present paper. In Refs. [21,22], the tracer diffusion of a single particle on a heterogeneous surface was studied. The substrate was simulated in the framework of a self-consistent description, where site-saddle-point energy correlations were involved in a general way. The influence of heterogeneity and correlations on the dynamic of migration was analyzed. Later, Bulnes et al. [23] studied the collective diffusion of adsorbed particles on correlated heterogeneous surfaces. The surface heterogeneity was introduced through the dual site–bond model (DSBM). The DSBM [5] describes the adsorptive energy through a site f_S, and a bond f_B distribution, and a construction principle: the adsorptive energy of any site must be bigger than that of any of the bonds connected to that site. According to the degree of overlapping between the two distributions, f_S and f_B, different topographies can be generated. The authors showed that the coverage dependence of the transport coefficients is strongly affected by that overlapping.

The energetic topography shown, for example, by the DSBM as a collection of random shaped patches, suggests the idea of representing a heterogeneous surface by patches of different adsorptive energy characterized by a typical length scale l (patch size). Some developments in the theory of adsorption on heterogeneous surfaces, like the supersite approach [24], and experimental advances in the tailoring of nanostructured adsorbates [25,26] encourage this kind of study. A special class of bivariate surfaces, with a chessboard structure, has been observed to occur in a natural system [27]. Bivariate surfaces may also mimic, to a rough approximation, more general heterogeneous surfaces with energetic topography arising from a solid where a small amount of randomly distributed impurity (strongly adsorptive) atoms are added [28]. In this case the energetic topography could be roughly represented by a random spatial distribution of irregular patches (with a characteristic size) of weak and strong sites.

In this context, simple heterogeneous surfaces, characterized by two kinds of nonequivalent sites, have also been intensively used in modeling adsorption [29–33] and surface diffusion phenomena [34–44]. In the first case, adsorption on bivariate surfaces with square patches and strip topographies has been studied through Monte Carlo simulations for adparticles with nearest-neighbor interaction energy, at a fixed temperature [29,30]. Later, the study was extended to include the effects of temperature on the adsorption process [31]. It was found that both the adsorption isotherms and the differential heat of adsorption follow scaling laws involving the patch size l with a universal exponent, and that this characteristic length defining the topography could, in principle, be obtained from the analysis of experimental results [32,33].

On the other hand, collective diffusion coefficients for bivariate surfaces with different topographies were studied by using MC simulations [34–36]. Even though the consequences of introducing lateral interactions were analyzed, the small magnitude of these couplings did not allow to obtain a complete description of the combined effect of surface topography and ad–ad interactions. The diffusion of particles on heterogeneous lattices with two kinds of nonequivalent sites has also been investigated by theoretical approaches such as statistical models [37,41] and real-space renormalization group (RSRG) method [42,43]. In all cases, interesting results were obtained and compared with MC and experimental data.

Following the line of the studies mentioned in previous paragraph, the scope of the present work is to determine, via MC simulation, the general properties of the diffusion of interacting particles on model bivariate surfaces with a characteristic correlation length, l. Here we will try to demonstrate that numerical simulations, combined with a correct theoretical interpretation of the results, can be very useful to obtain a very reasonable description of the diffusion of interacting particles on surfaces with different topographies. The work is organized as follows: In Section 2, a model of a generalized heterogeneous surface with a discrete adsorption energy distribution is presented. The general basis of the MC simulation of adsorption and diffusion are outlined in Sections 3.1 and 3.2, respectively. Results are presented in Section 4. Finally, general conclusions are given in Section 5.

2. Model

The adsorption of simple particles on a two-dimensional heterogeneous bivariate lattice is considered. The substrate is represented by a square lattice of $M = L \times L$ adsorptive sites with periodical boundary conditions. Heterogeneity is introduced by considering deep and shallow adsorptive sites, with two possible adsorption energies given by ε_D and ε_S, respectively. In addition, $\Delta\varepsilon = \varepsilon_D - \varepsilon_S$, where ε_S can be taken equal to zero without loss of generality. These sites are spatially distributed forming patches of size $l \times l$, as shown in Fig. 1(a).

In order to describe the system of N particles adsorbed on M sites (each site can only be empty or occupied by a single particle) at a given temperature T, we use the occupation variable c_i (equal to zero when site i is empty or equal to 1 when occupied) and define the Hamiltonian of the system as,

$$H = w \sum_{(i,j)} c_i c_j + \sum_{i=1}^{M} c_i \varepsilon_i - \mu \sum_{i=1}^{M} c_i, \tag{1}$$

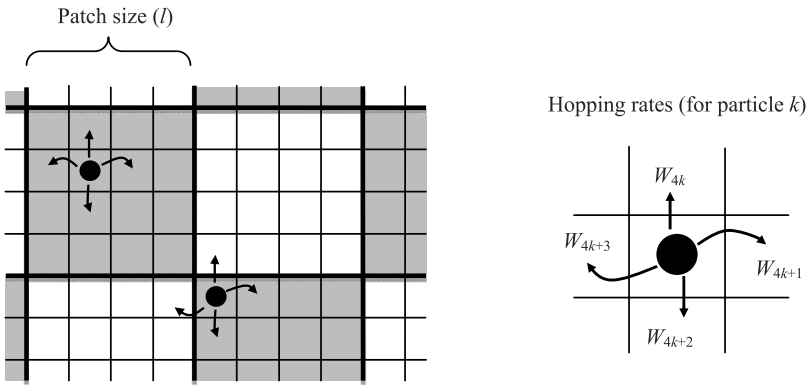

Fig. 1. (a) Patchwise distribution of deep (gray) and shallow (white) sites, for a patch size of $l = 4$. One particle is in the inner of a deep patch and the other is located in the border (corner) of a patch. (b) Hopping rates associated to the particle k.

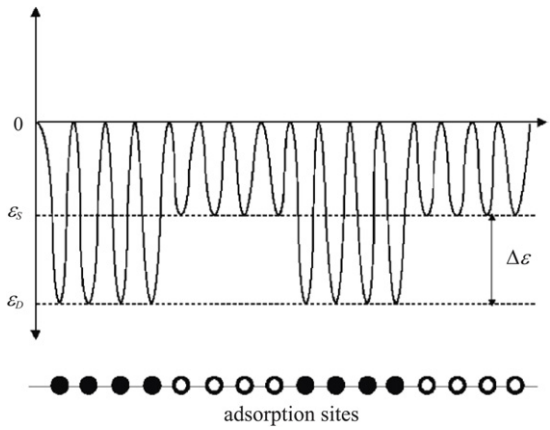

Fig. 2. Schematic representation of a one-dimensional bivariate surface with patchwise topography. The filled (empty) circles represent the deep (shallow) sites with energy $\varepsilon_D(\varepsilon_S)$. The patch size in the figure is $l = 4$.

where w is the lateral interaction energy among nearest neighbor (NN) particles, (i, j) represent all pairs of NN sites, and μ is the chemical potential.

We consider particles that can jump to NN empty sites (Fig. 1(b)) only through activated transitions, where the transition rate depends only on the initial particle configuration energy and the barrier potential between sites, which is essentially the adsorption energy of the site (see Fig. 2).

In the kinetic Monte Carlo (kMC) framework, for the accounting of all the possible hopping cases we have to consider the hopping from an occupied (•) to an empty (○) NN site when this pair of sites is immersed in all the possible environments, even considering the heterogeneity of the surface. To be specific, we define the following hopping rates for a (•○) pair of sites immersed in an environment x:

$$W_{\bullet\circ,x} = v \exp\left[-\left(\varepsilon_x^* - \varepsilon_{\bullet\circ,x}\right)/k_B T\right] \tag{2}$$

where v is a pre-exponential factor, $\varepsilon_{\bullet\circ,x}$ is the energy of the (•○) pair in the environment x, ε_x^* accounts for the interaction with the substrate and k_B is the Boltzmann constant.

3. Monte Carlo simulations

3.1. Adsorption

For heterogeneous systems exact analytical solutions are not available and some other convenient method, like MC simulation, must be used. The adsorption process is conveniently simulated in the Grand Canonical Ensemble [44]. For a given value of the temperature and the chemical potential, an initial configuration with $N = M/2$ particles adsorbed at random positions is generated. Then, an adsorption–desorption chain of events is started by choosing a site at random and attempting to change its occupancy number according to the Metropolis transition probability [45],

$$P = \min\left\{1, \exp\left(-\frac{\Delta H}{k_B T}\right)\right\}, \tag{3}$$

where $\Delta H = H_f - H_i$ is the difference between the Hamiltonians of the final and initial states. A MC step (MCS) is achieved when M sites have been tested to change their occupancy state. The approximation to thermodynamic equilibrium is monitored through the fluctuations in the number N of adsorbed particles; this is usually reached in about 10^5 MCS. After that, averages are taken on the system through the next 10^5 MCS on non-correlated configurations. At high values of w/k_BT up to 10^6 MCS had to be used in order to let the system to relax from metastable states.

Thermodynamic quantities such as the mean coverage θ, and the mean energy U, are obtained as simple averages,

$$\theta = \frac{\langle N \rangle}{M} = \frac{1}{M}\sum_{i=1}^{M} \langle c_i \rangle , \qquad U = \langle H \rangle , \tag{4}$$

where the bracket denotes average over n uncorrelated configurations. The thermodynamic factor, T_h, is calculated through the average [34],

$$T_h = \left[\frac{\langle N^2 \rangle - \langle N \rangle^2}{\langle N \rangle} \right]^{-1} . \tag{5}$$

T_h can also be written in terms of derivatives of the chemical potential with respect to surface coverage. Namely,

$$T_h = \left[\frac{\partial \left(\mu / k_B T \right)}{\partial \ln \theta} \right]_T . \tag{6}$$

3.2. Diffusion

The method for determining the collective diffusion coefficient, $D(\theta)$, is based on the Kubo–Green equation which we write here as [46–48],

$$D(\theta) = D_J(\theta) \left(\frac{\partial \mu / k_B T}{\partial \ln \theta} \right)_T . \tag{7}$$

D_J denotes the so-called jump diffusion coefficient, which is related with the individual movement of the whole set of diffusion particles (or their center of mass),

$$D_j(\theta) = \lim_{t \to \infty} \left\{ \frac{1}{2t} \left\langle \frac{1}{N} \left(\sum_{i=1}^{N} \Delta \vec{r}_i(t) \right)^2 \right\rangle \right\} , \tag{8}$$

where $\Delta \vec{r}_i(t)$ denotes the ith particle's displacement at time t. D_J is, in general, dependent on the concentration (coverage). For the diffusion of simple (monomeric) particles in two dimensions it is known that $\left\langle \frac{1}{N} \left(\sum_{i=1}^{N} \Delta \vec{r}_i(t) \right)^2 \right\rangle = \left\langle R^2(t) \right\rangle \propto t$ in the limit of long times, so that jump coefficient can be easily obtained from simulation through,

$$D_J(\theta) = \lim_{t \to \infty} \frac{\left\langle R^2(t) \right\rangle}{2t} . \tag{9}$$

On the other hand, the collective diffusion coefficient, D, also known as chemical diffusion, is related with the phenomenological description of the diffusion process from Fick's law. The proportionality factor in Eq. (7) is the already defined thermodynamic factor, T_h, which is obtained, in the context of an adsorption process in the grand canonical ensemble, as the derivative of the concentration with respect to the chemical potential or from the fluctuations of N (see Eq. (5)).

Our numerical simulations are performed by considering a fast kMC scheme based on the n-fold way-like algorithm [20], which relies on the exact computation of the transition probabilities from each configuration of the system and the association of the time evolution to a random variable sampled from the waiting time distribution for these configurations. Therefore, the kMC simulation of the diffusion process is performed by iterating the following two steps for any given configuration:

(i) The transition probabilities (or hopping rates) W_i ($i = 1, 2, \ldots, 4N$), where $4N$ represents the accounting for the four possible transitions (left, right, up and down) for each of the particles, are evaluated by using Eq. (2). Then, a random number ξ_1 uniformly distributed in [0, 1) is obtained and the kth event chosen from the condition,

$$\frac{1}{W}\sum_{i=1}^{k-1} W_i < \xi_1 \leq \frac{1}{W}\sum_{i=k}^{4N} W_i ; \quad W = \sum_{i=1}^{4N} W_i , \tag{10}$$

is performed.

(ii) A second random number ξ_2 is generated and the time t elapsed from the initial state is incremented through,

$$t^{new} \leftarrow t^{old} + \Delta T = t^{old} - \frac{1}{W} \ln \xi_2 . \tag{11}$$

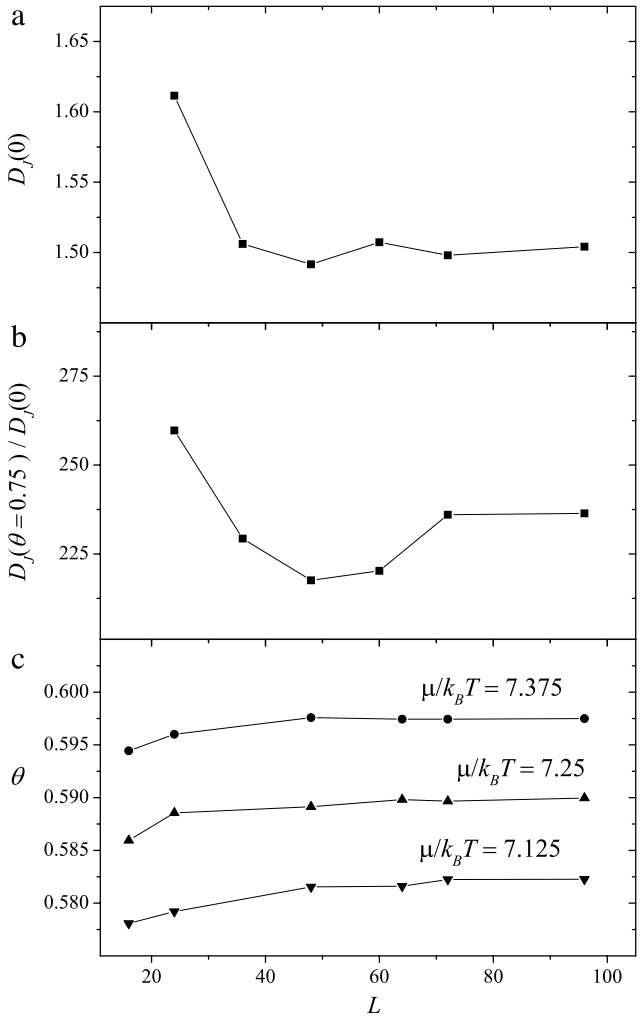

Fig. 3. Jump diffusion coefficient as a function of the system size L, for $\Delta\varepsilon = 6,\ w = 3$ and $l = 4$ at the limit of zero coverage (a), and at $\theta = 0.75$ (b). In the case the adsorption isotherms, the coverage as a function of the system size is shown in (c) for three different values of chemical potential. As it can be observed, finite-size effects are negligible for $L > 72$.

The advantages of using the n-fold way MC scheme described above can be understood by taking into account that in a standard MC simulation framework the number of trials for a successful jump scales as a function of time as $1/W_i$, while the efficiency of the kMC is not affected by an increase in w/k_BT or ε_i/k_BT, since every trial produces a successful jump of some particle to a NN empty site.

4. Results and discussion

The computational simulations have been developed for square $L \times L$ lattices with $L = 96$ and periodic boundary conditions. The finite-size effects on the adsorption and diffusion properties were investigated by considering systems of increasing sizes (ranging between $L = 12$ and $L = 96$). As an example of such studies, Fig. 3 shows, for a typical case ($\Delta\varepsilon = 6,\ w = 3$ and $l = 4$), how the jump diffusion coefficient varies with the lattice size (Fig. 3(a) and (b)) for a coverage of $\theta = 0.75$. For the adsorption process, the coverage as a function of the system size is analyzed, for the same case, at three different values of chemical potential (Fig. 3(c)). As it can be observed, finite-size effects are negligible for $L > 72$. The linear dimension L has to be properly chosen such that the adlayer structure is not perturbed, that is, L must be even and multiple of l. The system size values used in Fig. 3 are $L = 12$; 24; 36; 48; 60; 64; 72 and 96.

In the present study, we focus on the case of repulsive interaction energy among adsorbed particles ($w \geq 0$). This is far more interesting since, as we shall see, order–disorder phase transitions can take place in the adsorbate, even if the order can be partially disturbed by heterogeneity [29].

As a basis for discussing the effects of heterogeneity, we begin by briefly reviewing the results corresponding to the particular case of a homogeneous substrate ($\Delta\varepsilon = 0$). The coverage dependence of the chemical potential (adsorption

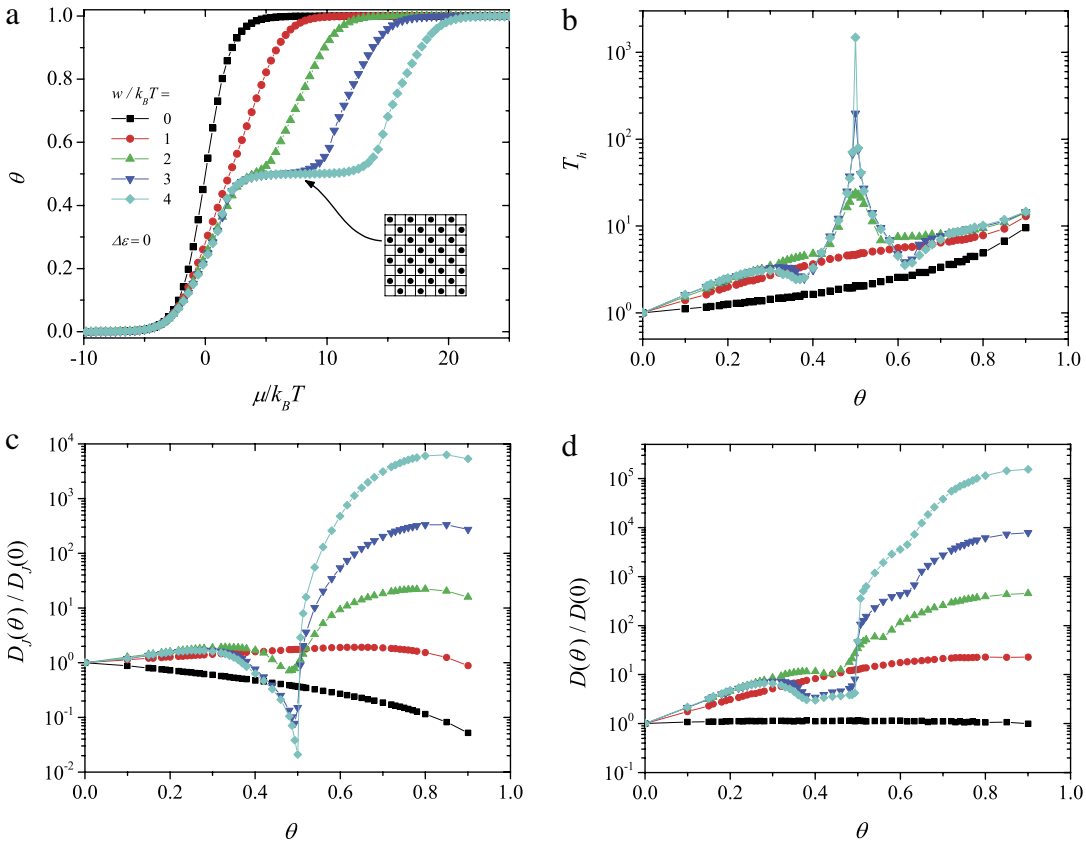

Fig. 4. Adsorption isotherms (a), thermodynamic factor (b), jump diffusion coefficient (c) and collective diffusion coefficient (d) for interacting particles (as indicated) adsorbed on a homogeneous surface.

isotherm) and the thermodynamic factor are shown in Fig. 4(a) and (b), respectively, for increasing values of the interaction energy w. As expected for this system, the adsorption isotherms develop a pronounced plateau at $\theta = 1/2$ as w/k_BT increases, accompanied by a sharp peak in the thermodynamic factor. This singularity corresponds to the formation of a $c(2 \times 2)$ phase on the surface (see inset of Fig. 4(a)). The presence of this structure strongly restricts the mobility of the ad-particles and, as shown in Fig. 4(c), the normalized jump diffusion coefficient $D_J(\theta)/D_J(0)$, presents a marked minimum at the same critical coverage value.

The combination of the effects just discussed for T_h and $D_J(\theta)$ produces the behavior of the normalized collective diffusion coefficient $D(\theta)/D(0)$, shown in Fig. 4(d). As can be observed for $w/k_BT = 0$, $D(\theta)/D(0)$ remains constant and equal to 1 in the entire range of coverage. For low values of w/k_BT (≤ 1), the repulsive interactions favor the mobility of the ad-particles and collective diffusion coefficient increases with coverage. As w/k_BT increases, the collective diffusion coefficient increases with θ, shows a local maximum around $\theta \approx 1/4$ and, due to the formation of the $c(2 \times 2)$ ordered phase, the mobility decreases to a wide minimum in the range $0.4 \leq \theta \leq 0.5$. For $\theta > 0.5$, the breaking of the ordered structure increases the number of (unstable) available configurations, and consequently, the mobility of the adsorbed particles is also greatly increased. This effect is observed in both diffusion coefficients with an abrupt initial increase from the minimum, and then a slower increase reaching the limit of full coverage. As mentioned above, repulsive interactions favor the diffusion and, consequently, the value of $D(\theta \to 1)/D(0)$ increases as w/k_BT is increased.

Proceeding to a more complex situation, Fig. 5 shows the adsorption isotherms (a), thermodynamic factor (b), jump diffusion coefficient (c) and collective diffusion coefficient (d) for a fixed topography (chessboard patches with $l = 4$), $w/k_BT = 4$ and different values of $\Delta\varepsilon/k_BT$. As a general feature, the shapes of adsorption isotherms (Fig. 5(a)) change from showing one plateau at $\theta = 1/2$ for $\Delta\varepsilon/k_BT = 0$, up to three plateaus at coverage 1/4, 1/2 and 3/4 for $\Delta\varepsilon/k_BT = 8$. It is interesting to note that the central plateau for $\Delta\varepsilon/k_BT = 0$ is due to repulsive interactions (the formation of a $c(2 \times 2)$ ordered phase) while for $\Delta\varepsilon/k_BT = 8$ it is a combined effect of heterogeneity and lateral interactions. In fact, in the case of $\Delta\varepsilon/k_BT = 8$ the filling of the lattice now proceeds according to the following processes: (i) the deep site patches are filled until the $c(2 \times 2)$ ordered phase is formed on them (see inset in Fig. 5(a)); (ii) since $\Delta\varepsilon < 4w$, the shallow site patches are filled until the $c(2 \times 2)$ ordered phase is formed on them (see inset in Fig. 5(a)); (iii) the filling of the deep site patches is completed (see inset in Fig. 5(a)); and (iv) the filling of the shallow site patches is completed (see inset in Fig. 5(a)). As in Fig. 4, each plateau in the adsorption isotherm is accompanied by a marked peak in the thermodynamic factor (Fig. 5(b)).

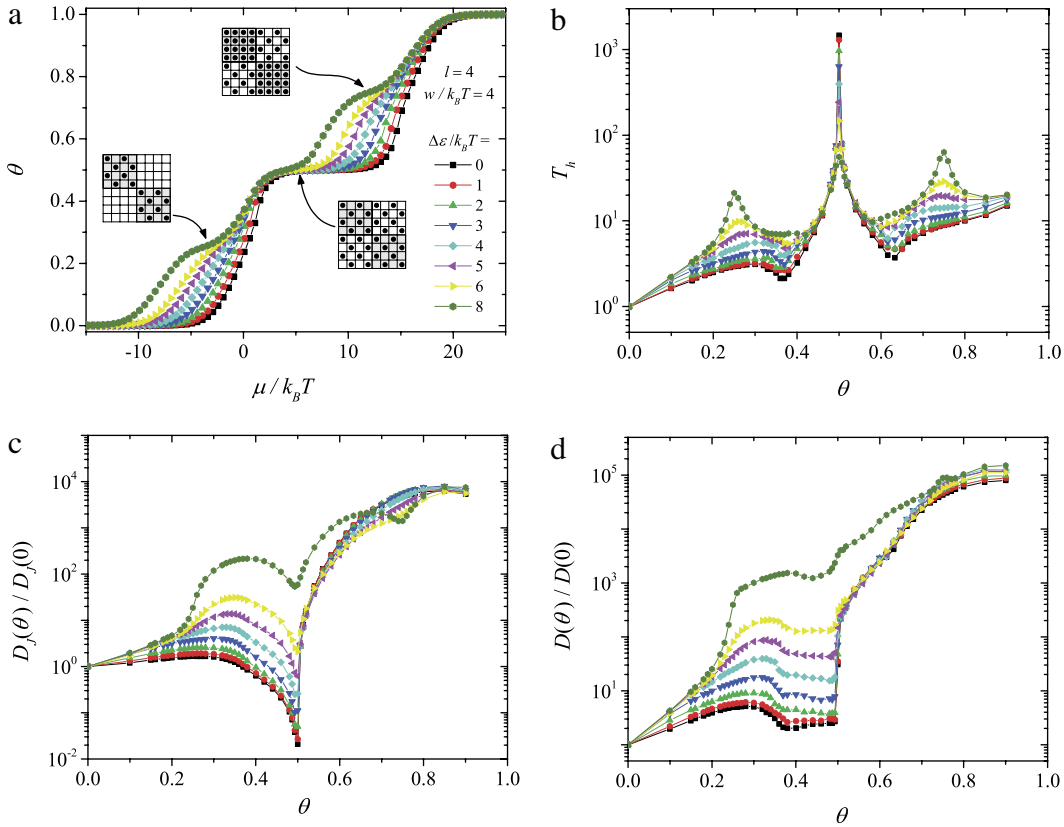

Fig. 5. The same as Fig. 4 for a fixed topography (chessboard patches with $l = 4$), $w/k_BT = 4$ and different values of $\Delta\varepsilon/k_BT$.

In the case of the jump diffusion coefficient (Fig. 5(c)), all curves show a sharp minimum at half coverage and develop a second local minimum at $\theta = 3/4$ as $\Delta\varepsilon/k_BT$ is increased. However, it is interesting to observe that the $D_J(\theta)/D_J(0)$ curves do not show a minimum at $\theta = 1/4$. This can be explained given that for large values of $\Delta\varepsilon$ the deep patches are first filled forming the ordered phase $c(2 \times 2)$, and the shallow ones, that remain mostly empty at this coverage, allow a sharp increase in the mobility of the new particles. An important conclusion can be drawn from Fig. 5. Namely, the presence of ordered structures in the adsorbate is directly related to the formation of plateaus in the adsorption isotherms (peaks in the thermodynamic factor). However, not always the existence of order in the adlayer provides a corresponding minimum in the jump diffusion coefficient.

To conclude with the analysis of Fig. 5, the collective diffusion coefficient is shown in part d. The sharp minimum at $\theta = 1/2$ observed in $D_J(\theta)/D_J(0)$ is no longer present in the case of $D(\theta)/D(0)$. Neither shows any indication of minimum at $\theta = 3/4$. This behavior can be explained from Eq. (7), which shows that the collective diffusion coefficient (Fig. 5(d)) is the product of the jump diffusion coefficient (Fig. 5(c)) and the thermodynamic factor (Fig. 5(b)). Thus, each minimum in $D_J(\theta)$ is accompanied by a maximum in T_h and the corresponding $D(\theta)$ is a smooth function in all range of coverage.

Fig. 6 shows the case of a large patch energy difference, $\Delta\varepsilon/k_BT = 8$, $l = 4$ and different values of w/k_BT. The behavior of the adsorption isotherms (Fig. 6(a)) can be explained as follows. The case $w/k_BT = 4$ was already discussed in Fig. 5. As w/k_BT diminishes, the filling process occurs in the following way: (i) deep site patches are filled first up to $\theta = 1/4$, where a $c(2 \times 2)$ structure is formed on them; (ii) the filling of deep site patches is completed up to $\theta = 1/2$; processes (iii) and (iv) are equivalent to processes (i) and (ii) for shallow site patches. As it can be easily understood, as long as the condition $\Delta\varepsilon > 4w$ is satisfied, the adsorption process is similar to the one described above, i.e., deep site patches are filled first and shallow site patches are filled after (see insets in Fig. 6(a)).

An interesting effect can be observed in the normalized jump diffusion coefficient, Fig. 6(c). First, in absence of lateral interaction ($w/k_BT = 0$) the curve presents a minimum at coverage $\theta = 1/2$ which is essentially due to the presence of surface heterogeneity as particles tend to occupy first the sites belonging to the deep patches. As these sites become scarcer as we approach this coverage, the mobility of the adparticles is strongly reduced. For increasing lateral interaction, the ordered phase $c(2 \times 2)$ is favored in the deep patches along with a premature population (starting at $\theta = 1/4$) of the shallow ones, increasing at this point the general mobility. This explains the disappearing of the minimum in the curves for intermediate values of w/k_BT. Finally, at higher values of w/k_BT, the curves present again various minimums corresponding

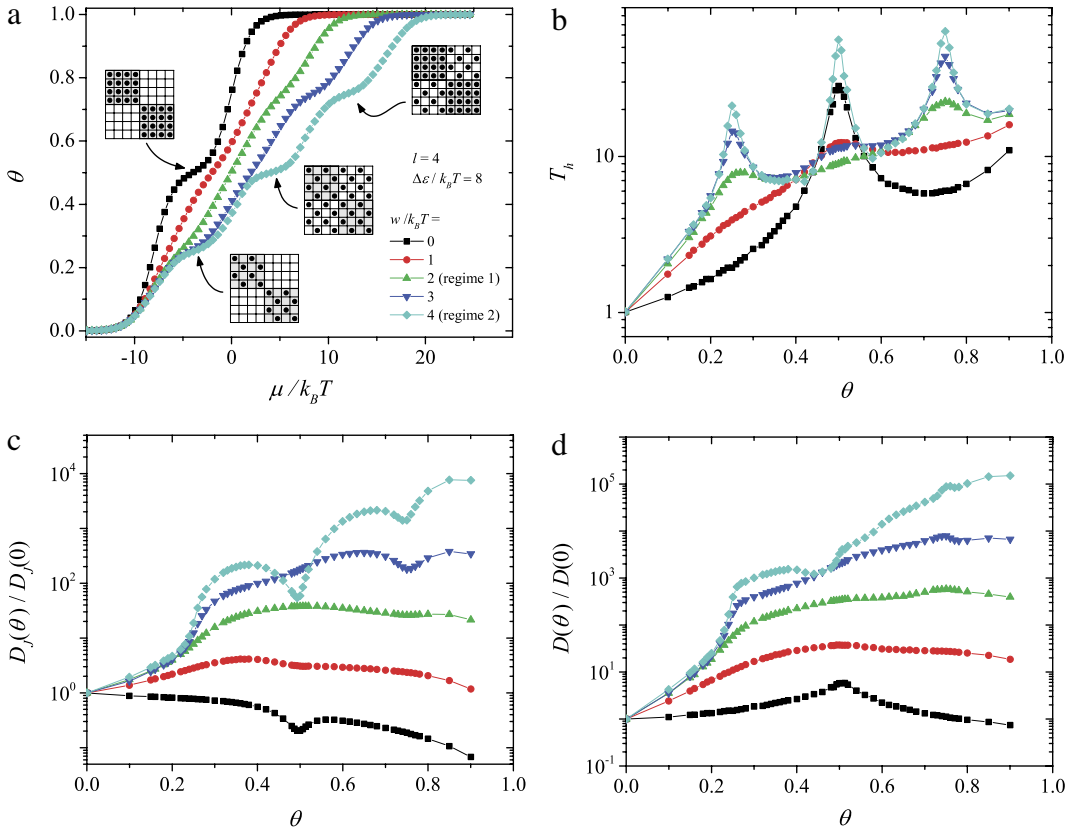

Fig. 6. The same as Fig. 4 for $\Delta\varepsilon/k_BT = 8$, $l = 4$ and different values of w/k_BT.

to the different regimes also observed in the adsorption isotherms, this time related to both surface heterogeneity and lateral interaction, which is responsible for the formation of ordered structures $c(2 \times 2)$ on the patches.

Fig. 6(d) shows the collective diffusion coefficient obtained from the Kubo–Green Eq. (7). As this quantity accounts for both the mobility and the adsorption–desorption process present in the thermodynamic factor shown in Fig. 6(b), it is expected to have some differences in the behavior. Starting by the non-interacting case, $w/k_BT = 0$, there is a maximum at half coverage instead of the minimum observed in the jump diffusion. For intermediate values of w/k_BT the curves have no special details at the critical coverage although, at higher values of w/k_BT, the minimum at $\theta = 1/2$ is recovered again.

Figs. 7 and 8 are intended to show the topography effects on the diffusion coefficients. The curves correspond to various sizes l, considering both ordered patches forming a chessboard, as well as randomly distributed patches. A large energy difference, $\Delta\varepsilon/k_BT = 8$, is considered together with two cases: no lateral interaction, $w/k_BT = 0$ (Fig. 7) and $w/k_BT = 4$ (Fig. 8).

In the case of no lateral interactions, the isotherms are not able to show any difference for the various topographies considered, as can be seen in Fig. 7(a) and (b). On the other hand, the jump diffusion curves for ordered patches (corresponding to full symbols in Fig. 7(c)) increase monotonically with the patch size along all the coverage axis and present a minimum at $\theta = 1/2$, as was already observed in Fig. 6. The same happens in the case of random distributed patches (curves with hollow symbols), although in this case they start higher than the ordered cases, for the same patch size.

Considering now lateral interactions $w/k_BT = 4$ the curves display features associated to the formation of ordered $c(2 \times 2)$ structures in the adsorbate at the critical densities. The isotherms in Fig. 8(a) present three plateaus, although they practically have no dependence with the topography. The jump diffusion curves in Fig. 7(c) present a step at $\theta = 1/4$ and minima at $\theta = 1/2$ and 3/4, in accordance with Figs. 5 and 6, showing a slight dependence with the patch size that increases with coverage. In the case of random distributed patches (hollow symbols), the curves start higher than the ordered cases, for the same patch size. In addition, the behavior of a random topography of size l seems to approach that of a chessboard topography with an effective size $l_{eff} > l$. From figure it is possible to draw a correspondence relation $l_{ordered} \approx 2\, l_{random}$, to obtain the equivalent curve between the ordered and the random patch situation. This relation has also been observed for the adsorption isotherms and can be explained from the distribution of pairs of nearest-neighbor sites in the substrate (shallow–shallow, deep–deep, shallow–deep). Interested readers are referred to Ref. [29] for a more complete description of this effect.

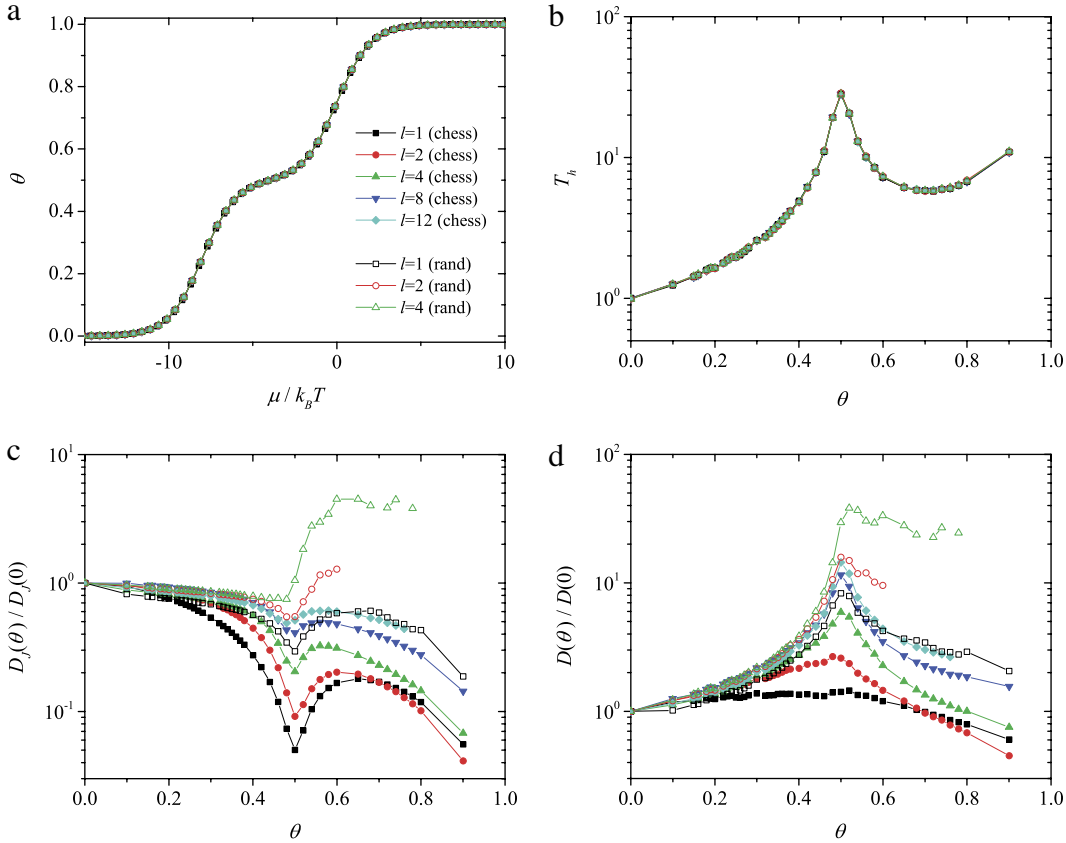

Fig. 7. The same as Fig. 4 for $\Delta\varepsilon/k_BT = 8$, $w/k_BT = 0$ and different topographies as indicated.

Finally, it is interesting to analyze the limit of small patches ($l = 1$). In the first place, the plateau in the isotherm at $\theta = 1/4$ is not present at all, which can be explained because in this case there is no room in the deep patches for the formation of a $c(2 \times 2)$ structure. Furthermore, this is the only case where the topography affects directly each NN transition, impacting heavily in the mobility and, consequently, in the diffusion coefficient. Since also the NN interactions are affected, the system behaves like a no lateral interaction case, as can be seen in the first part of the collective diffusion curve in Fig. 7(d).

5. Conclusions

In this paper, we have studied the diffusion of interacting particles adsorbed on heterogeneous bivariate substrates characterized by different energetic topographies. The heterogeneity is determined by two parameters: the difference of adsorptive energy between deep and shallow sites, $\Delta\varepsilon$, and an effective correlation length, l, representing the length scale for homogeneous adsorptive patches. We have considered, in particular, the case of repulsive interactions between adparticles and activated transitions in the diffusion process.

An interesting behavior is observed at low temperatures; in fact, the repulsive interactions induce a well-defined ordered structure in the adsorbed phase. The ordered phase corresponds to a $c(2 \times 2)$ structure and, depending on the ratio $\Delta\varepsilon/w$, two distinct filling regimes are clearly identified in the adsorption process. For $\Delta\varepsilon/w > 4$, the following sequence is observed: (i) deep site patches are filled first up to $\theta = 0.25$, where a $c(2 \times 2)$ structure is formed on them; (ii) the filling of deep site patches is completed up to $\theta = 0.50$; processes (iii) and (iv), corresponding to the regions $0.5 < \theta < 0.75$ and $0.75 < \theta < 1$, respectively, are equivalent to processes (i) and (ii) for shallow site patches. On the other hand, in the case $\Delta\varepsilon/w < 4$, (i) the deep site patches are filled until the $c(2 \times 2)$ ordered phase is formed on them; (ii) the shallow site patches are filled until the $c(2 \times 2)$ ordered phase is formed on them; (iii) the filling of the deep site patches is completed; and (iv) the filling of the shallow site patches is completed.

The existence of structures in the adlayer has appreciable effects on the adsorption isotherms with the formation of plateaus, accompanied by sharp peaks in the thermodynamic factor. These singularities in the adsorption quantities do not have a good sensitivity to surface heterogeneity and lateral interactions. In other words, it is not possible to distinguish if a plateau in the adsorption isotherm (peak in the thermodynamic factor) is a consequence of lateral couplings or heterogeneity.

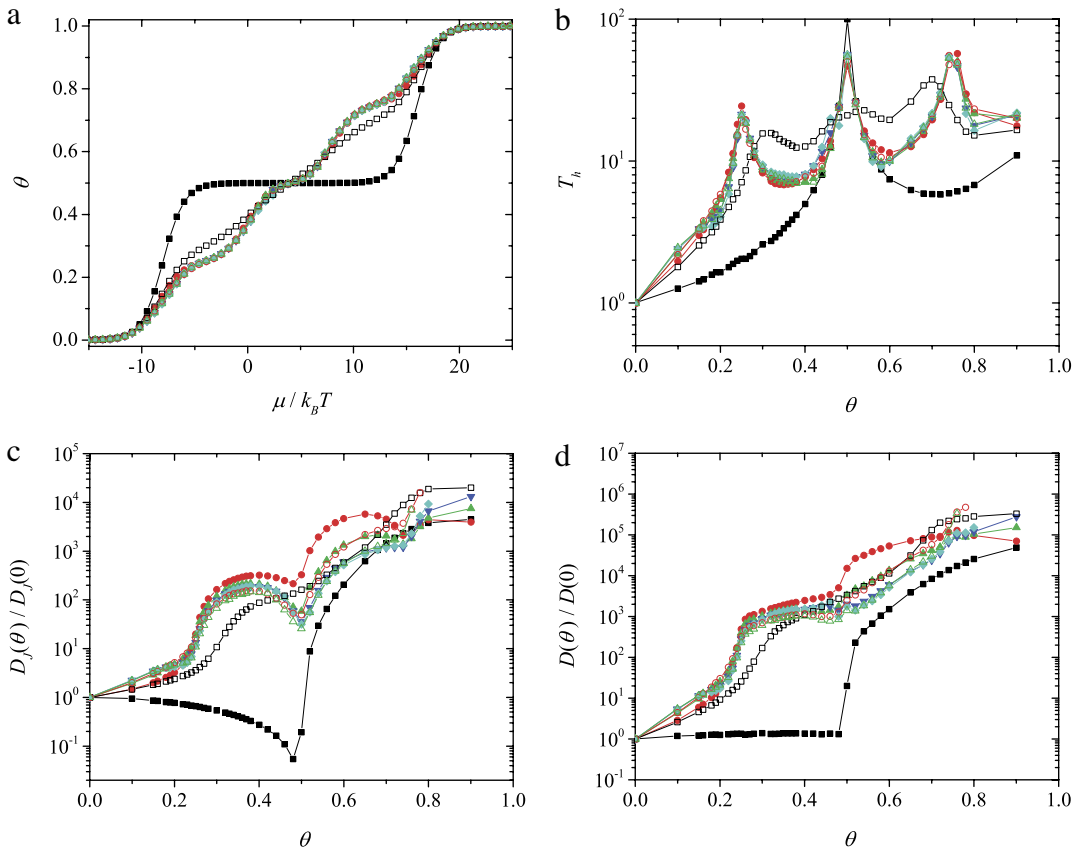

Fig. 8. The same as Fig. 5 for $\Delta\varepsilon/k_BT = 8$, $w/k_BT = 4$ and different topographies as indicated.

On the other hand, the diffusion coefficients have a more complex behavior. Even though the mobility of the adparticles is strongly affected in the presence of highly correlated ordered phases, the combination of lateral interactions and surface heterogeneity has varied effects on the diffusion quantities. In fact, in the case of homogeneous surfaces and strong repulsive lateral interactions, the presence of structures in the adlayer strongly restricts the mobility of the ad-particles and the diffusion coefficients present marked minimums at certain critical coverage values. The situation is different when the surface is constituted by patches of different energies. Under these conditions, when an ordered phase is formed on a patch, the existence of other empty patches allows a sharp increase in the mobility of the new particles and, consequently, a marked jump appears in the diffusion constants. Therefore, the existence of order not always provides a minimum in the diffusion coefficients in the presence of heterogeneity.

With respect to the topography, the obtained results from the transport coefficients show that random and ordered topographies are seen to behave in a similar way with a particularly interesting feature: the behavior of random topography of size l seems to approach that for ordered topography with an effective size $l_{eff} > l$ ($l_{ordered} \approx 2\, l_{random}$).

The kind of study presented here may be helpful in analyzing experimental data of a class of heterogeneous surfaces which can be approximately represented as bivariate surfaces.

Acknowledgments

This work was supported in part by CONICET (Argentina) under project number PIP 112-201101-00615; Universidad Nacional de San Luis (Argentina) under project 322000; and the National Agency of Scientific and Technological Promotion (Argentina) under project PICT-2010-1466.

References

[1] W. Rudzinski, D.H. Everett, Adsorption of Gases on Heterogeneous Surfaces, Academic Press, New York, 1992.
[2] W. Rudzinski, W.A. Steele, G. Zgrablich (Eds.), Equilibria and Dynamics of Gas Adsorption on Heterogeneous Solid Surfaces, Elsevier, Amsterdam, 1997.
[3] J. Tóth, Adsorption: Theory, Modeling, and Analysis, Dekker, New York, 2002.
[4] J. Keller, R. Staudt, Gas Adsorption Equilibria: Experimental Methods and Adsorption Isotherms, Springer, Boston, 2005.
[5] V. Mayagoitia, F. Rojas, V. Pereyra, G. Zgrablich, Surf. Sci. 221 (1989) 394.

[6] H. Jobic, in: H.G. Karge, J. Weitkamp (Eds.), Adsorption and Diffusion, Springer-Verlag, Berlin, Heidelberg, 2008.
[7] P.L. Krapivsky, S. Redner, E. Ben-Naim, A Kinetic View of Statistical Physics, Cambridge University Press, Cambridge, UK, 2010.
[8] M.A. Załuska-Kotur, Appl. Surf. Sci. 304 (2014) 122.
[9] M. Mińkowski, M.A. Załuska-Kotur, Appl. Surf. Sci. 304 (2014) 81.
[10] L. Padilla, H.O. Mártin, J.L. Iguain, Phys. Rev. E 82 (2010) 011124.
[11] L. Padilla, H.O. Mártin, J.L. Iguain, Phys. Rev. E 86 (2012) 011106.
[12] T. Becker, K. Nelissen, B. Cleuren, B. Partoens, C. Van den Broeck, Phys. Rev. Lett. 111 (2013) 110601.
[13] A.J. Ramirez-Pastor, M. Nazzarro, J.L. Riccardo, V. Pereyra, Surf. Sci. 391 (1997) 267.
[14] A.J. Ramirez-Pastor, F. Romá, A. Aligia, J.L. Riccardo, Langmuir 16 (2000) 5100.
[15] F. Nieto, C. Uebing, Ber. Bunsenges. Phys. Chem. 102 (1998) 974.
[16] F. Nieto, A.A. Tarasenko, C. Uebing, Europhys. Lett. 43 (1998) 558.
[17] A.A. Tarasenko, L. Jastrabik, F. Nieto, C. Uebing, Phys. Rev. B 59 (1999) 8252.
[18] A.A. Tarasenko, L. Jastrabik, F. Nieto, C. Uebing, Phys. Chem. Chem. Phys. 1 (1999) 1583.
[19] A.A. Tarasenko, F. Nieto, C. Uebing, Phys. Chem. Chem. Phys. 1 (1999) 3437.
[20] F. Bulnes, V. Pereyra, J.L. Riccardo, Phys. Rev. E 58 (1998) 86.
[21] K. Sapag, V. Pereyra, J.L. Riccardo, G. Zgrablich, Surf. Sci. 295 (1993) 433.
[22] K. Sapag, F. Bulnes, J.L. Riccardo, V. Pereyra, G. Zgrablich, Langmuir 9 (1993) 2670.
[23] F. Bulnes, V. Pereyra, J.L. Riccardo, G. Zgrablich, J. Chem. Phys. 11 (1999) 5181.
[24] W.A. Steele, Langmuir 15 (1999) 6083.
[25] M.X. Yang, D.H. Gracias, P.W. Jacobs, G. Somorjai, Langmuir 14 (1998) 1458.
[26] G.P. Lopinski, D.D.M. Wayner, R.A. Wolkow, Nature 406 (2000) 48.
[27] T.W. Fishlock, J.B. Pethica, R.G. Eydell, Surf. Sci. 445 (2000) L47.
[28] F. Bulnes, F. Nieto, V. Pereyra, G. Zgrablich, C. Uebing, Langmuir 15 (1999) 5990.
[29] F. Bulnes, A.J. Ramirez-Pastor, G. Zgrablich, J. Chem. Phys. 115 (2001) 1513.
[30] F. Bulnes, A.J. Ramirez-Pastor, G. Zgrablich, Phys. Rev. E 65 (2002) 031603.
[31] F. Romá, F. Bulnes, A.J. Ramirez-Pastor, G. Zgrablich, Phys. Chem. Chem. Phys. 5 (2003) 3694.
[32] F. Bulnes, A.J. Ramirez-Pastor, G. Zgrablich, Langmuir 23 (2007) 1264.
[33] P.M. Centres, F. Bulnes, G. Zgrablich, A.J. Ramirez-Pastor, Adsorption 17 (2011) 403.
[34] C. Uebing, V. Pereyra, G. Zgrablich, Surf. Sci. 366 (1996) 185.
[35] F. Nieto, C. Uebing, V. Pereyra, R.J. Faccio, Surf. Sci. 423 (1999) 256.
[36] F. Nieto, C. Uebing, Physica A 276 (2000) 215.
[37] Z. Chvoj, H. Conrad, V. Cháb, M. Ondrejcek, A.M. Bradshaw, Surf. Sci. 329 (1995) 121.
[38] Z. Chvoj, H. Conrad, V. Cháb, Surf. Sci. 352 (1996) 983.
[39] Z. Chvoj, H. Conrad, V. Cháb, Surf. Sci. 376 (1997) 205.
[40] Z. Chvoj, V. Cháb, H. Conrad, Surf. Sci. 426 (1999) 8.
[41] Z. Chvoj, H. Conrad, V. Cháb, Surf. Sci. 442 (1999) 455.
[42] A. Tarasenko, L. Jastrabik, T. Müller, Phys. Rev. B 75 (2007) 085401.
[43] A. Tarasenko, L. Jastrabik, T. Müller, Phys. Rev. B 76 (2007) 134201.
[44] D. Nicholson, N.G. Parsonage, Computer Simulation and the Statistical Mechanics of Adsorption, Academic Press, London, 1982.
[45] N. Metropolis, A.W. Rosenbluth, M.N. Rosenbluth, A.H. Teller, E. Teller, J. Chem. Phys. 21 (1953) 1087.
[46] D.A. Reed, G. Erlich, Surf. Sci. 102 (1981) 588.
[47] D.A. Reed, G. Erlich, Surf. Sci. 105 (1981) 603.
[48] R. Gomer, Rep. Progr. Phys. 53 (1990) 917.